Probing the structure of gas expanded liquids using relative permittivity, density and polarity measurements

Andrew P. Abbott,* Eric G. Hope, Reena Mistry and Alison M. Stuart

Received 13th May 2009, Accepted 30th July 2009
First published as an Advance Article on the web 25th August 2009
DOI: 10.1039/b915570h

Gas expanded liquids (GXLs) have been shown to be useful solvents with interesting properties between those of liquids and supercritical fluids. In this work the physical properties of 15 fluids are quantified at 50 bar CO_2 pressure and 25 °C and the data were used to gain an insight into the bulk and local structure upon pressurisation. It is shown that high CO_2 solubilities can be obtained in all solvents except the higher alcohols. Density measurements show that upon pressurisation the free volume of most solvents increases by up to 10%. The Kamlet and Taft and E_T parameters for the expanded solvents show that preferential solvation of the indicator solute occurs but that the ratio of solvent in the cybotactic and bulk regions remain roughly constant at a given pressure.

Introduction

Gas expanded liquids (GXLs) are quite simply liquids 'expanded' with a gaseous co-solvent; *i.e.* a mixture of a pure gas and an organic solvent at pressure and temperature conditions which are below those of the critical point of the mixture. As pressure increases, gas concentration increases and solvent power is lowered. Operating conditions exceeding the critical point result in formation of a co-solvent modified supercritical (sc) fluid. Similar to their supercritical counterparts, the solvent power of GXLs can be tuned by varying the liquid phase concentration as a function of pressure. At the same time, the dissolved gas can modify the physical properties of the liquid or solvent, making it less viscous and thereby enhancing its mass transport properties.

The operating pressures for gas expanded systems are typically 30 to 80 bar, which are much lower than the pressures required for reaching the supercritical phase. This gives GXLs a practical advantage over comparable supercritical systems in terms of specialised equipment and the outlay associated with them. At the same time, in terms of solvent power and transportability when compared to gases and liquids, GXLs express more liquid-like characteristics than supercritical fluids.

Gas expanded liquids have been shown to have great potential for tunability when the possible combinations of solvent, expanding gas, and/or co-solvent are taken into consideration. Depending on the nature of the solvent media and the gas used, gas expansion has been shown to either increase solubility[1,2] (to induce miscibility more specifically for biphasic systems) or decrease solubility[3,4] (for applications in crystallisation, extraction or separation). Although CO_2 is the most commonly used gas for expansion, other compressed gases are also capable of acting as an expanding medium, such as ethane and nitrous oxide.[5] GXLs have found application in micronisation of chemical substances through a number of related techniques such as rapid expansion of supercritical solutions,[6–9,10] gas anti-solvent crystallisation,[10–13] aerosol solvent extraction systems[14] and particles from a gas saturated solution.[15] The other major application has been in the use of carbon dioxide expanded liquids (CXL) as replacement solvents for a variety of reactions at the laboratory scale, including oxidation, hydrogenation and hydroformylation which are covered in a number of recent reviews.[16–18]

In the current work, we study the physical properties of a number of GXLs expanded at constant pressure and volume using CO_2. Relative permittivity, density and polarity data are used to quantify the solubility of CO_2, the change in molar free volume and the local solvation in these systems.

Experimental

The high pressure optical cell used for solvatochromic studies was constructed from 316 stainless steel with 1 cm thick sapphire windows. The gas seals were made from Teflon. The cell path length was 6 cm and the cell volume was 70 cm^3. Light was fed into and out of the high-pressure cell by fibre-optic cables (Hellma, Müllheim, FRG) fitted with a 662 QX prism adapter. Pressure was applied using a model P50-series piston controlled pump (Thar Technologies Inc.; Pittsburg, PA, USA) and was monitored (± 2 bar) using a Swagelok manometer. The temperature of the cell was measured using an iron/constantan thermocouple, the tip of which was in contact with the solvent close to the centre of the cell. The temperature was held at a given value (± 0.5 K) using a CAL-9300 controlled heater. A Shimadzu Model UV-1601 Spectrophotometer was used to measure the solvatochromic shift of the different indicator dyes in the visible absorbance spectrum.

The relative permittivity data were obtained using a cell lined with a layer of Teflon (1 mm thick), and with an internal volume of 24.7 cm^3. An O-ring covered in Teflon was used to provide a high-pressure seal between the head and base of the cell and the electrical feedthroughs (RS Components Ltd.) employed were sealed with Swagelok fittings. Prior to each experiment the cell

Department of Chemistry, University of Leicester, Leicester, UK LE1 7RH. E-mail: Andrew.abbott@le.ac.uk; Fax: +44 116 252 3789

Table 1 Relative permittivity, density, E_T and π* values for 15 solvents at 1 and 50 bar CO_2 pressure at 25 °C

	ε		X_{CO_2}	ρ/g cm^{-3}		% V_{free}		π^*		E_T/kcal mol^{-1}	
P/bar	1	50	50	1	50	1	50	1	50	1	50
Cyclohexane	1.95	1.30	0.749	0.773	0.798	31.1	40.78	0.034	0.067	51.94	52.45
Toluene	3.00	1.78	0.637	0.865	0.885	28.6	34.18	0.503	0.177	49.83	51.40
Diethylether	4.86	2.50	0.626	0.708	0.793	36.4	38.72	0.266	0.043	50.93	52.00
THF	7.57	3.41	0.641	0.880	0.916	28.8	33.66	0.553	0.367	49.58	50.55
DCM	7.99	3.64	0.630	1.318	1.283	29.6	24.76	0.812	0.487	48.36	50.01
Acetone	20.79	8.20	0.639	0.787	0.855	31.8	36.7	0.677	0.432	49.11	50.11
MeCN	36.00	13.86	0.634	0.777	0.860	29.0	49.92	0.727	0.530	48.84	49.64
DMF	39.14	17.30	0.574	0.945	0.965	23.3	28.79	0.880	0.841	48.15	48.32
DMSO	49.67	21.01	0.590	1.096	1.092	21.8	25.41	1.039	0.938	47.33	47.87
MeOH	33.68	11.68	0.675	0.790	0.799	27.6	42.76	0.598	0.372	47.40	48.65
EtOH	25.78	8.86	0.685	0.786	0.822	28.9	39.99	0.537	0.291	47.40	49.22
n-PrOH	21.23	12.95	0.411	0.801	0.835	28	32.05	0.520	0.336	47.51	48.91
i-PrOH	20.62	12.40	0.421	0.782	0.794	29.9	35.70	0.482	0.346	47.81	48.81
n-BuOH	18.78	11.58	0.407	0.806	0.820	28.1	32.68	0.508	0.439	47.54	48.17
t-BuOH	13.49	10.37	0.251	0.783	0.796	30.4	32.45	0.407	0.373	48.38	48.59

was purged with the appropriate gas. The pressure was then applied using a model 10-500 pump (Hydraulic Engineering Corp.; Los Angeles, CA, USA) driven by compressed air and retained at a given value (± 2 bar) using a UCC type PGE 1001.600 manometer. The temperature of the cell was measured using an iron/constantan thermocouple, the tip of which was in contact with the solvent close to the centre of the cell. The temperature was held at a given value (± 0.5 K) using a CAL 9900 controlled heater. The cell consists of two rectangular stainless steel plates (attached to the electrical feedthroughs) with an area of 6.6 cm^2, held 1 mm apart by Teflon spacers.

The density data were determined using an Anton Paar DMA 512P densitometer and an Anton Paar mPDS 1000 evaluation unit designed to make measurements at both atmospheric and high pressures. The densitometer consists of a vibrating U-tube constructed from stainless steel with a volume of just a few cm^3 (occupied by the sample). The principle of the unit is based on the evaluation of the natural frequency of the electronic excitement of a tuning fork. The sample is placed inside a double steel-walled cylinder sealed at both ends, and the whole unit is thermostatted using an oil flow system which regulates the temperature to within one quarter of a degree. The electronic part of the unit involves a system which excites the tuning fork at constant amplitude and a frequency metre which records the time corresponding to a fixed number of periods.

Results and discussion

To characterise the effect of CO_2 pressurisation upon the properties of a solvent the relative permittivity was measured, and a range of organic solvents from nonpolar cyclohexane to polar DMSO were analysed. The cell capacitance was measured for each solvent and plotted against relative permittivity values reported in the literature. The calibration graph was used to calculate the relative permittivity of the CO_2 expanded solvents. The change in capacitance between the liquid solvent and its expanded equivalent was recorded and converted to the dielectric scale.

Fig. 1 and Table 1 shows the relative permittivity, ε_r, of a range of organic solvents, arranged in increasing polarity,

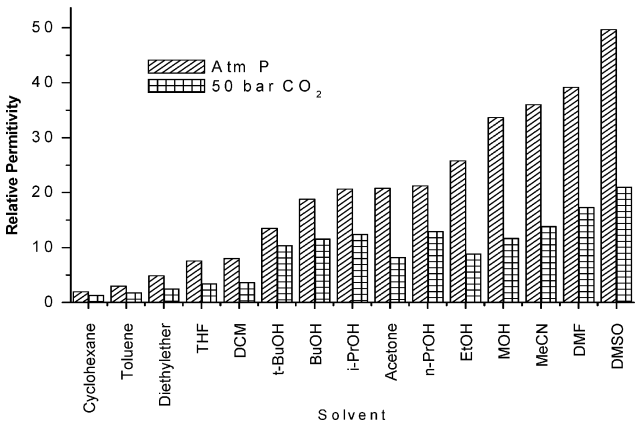

Fig. 1 The relative permittivity for a range of solvents and expanded solvents when pressurised with CO_2 at 50 bar pressure and 25 °C.

and the degree to which ε changes when they are expanded at 50 bar of CO_2 at ambient temperature. The relative permittivity values were obtained with an uncertainty of ± 2% and values obtained at ambient pressure were in good correlation with published data.[7] These results show that the relative permittivity of all the solvents decreased when expanded with CO_2, as would be expected. Generally, a greater change in permittivity was observed for the more polar solvents, with DMSO showing the largest change in dielectric constant when expanded, with its relative permittivity decreasing from 49 to 21. The magnitude of the changes in relative permittivity is surprising and shows that the dissolution of CO_2 into liquid organic solvents generates a substantial change in polarity from polar to nonpolar and it is this that has been utilised in many of the applications listed above.

Empirical observations demonstrate that not all solvents expand to the same extent when subjected to the same pressure of CO_2, and the differences result from the varied solubility of CO_2 in the liquid solvents. In this regard, CO_2 solubility in organic solvents has been reported by various authors, but there is no general method by which gas solubility can be predicted and large discrepancies have been reported between experimental and calculated solubilities. Several authors have adopted a

semi-empirical approach based on regular solution theory which, despite certain limitations, has become well accepted.[19–25] The dielectrometry technique[26–28] is a quick, simple and precise *in situ* technique that can be applied in pressurised solvents to measure the solubility of both polar and nonpolar liquid and solid solutes, which has been applied in a few cases for solubility measurements in sc fluids. The technique should also be applicable to determine the solubility of CO_2 in expanded solvents since;

$$\varepsilon_{mix} = \varepsilon_{CO_2} X_{CO_2} + \varepsilon_{solv} X_{solv} \quad (1)$$

where; ε_{mix} is the relative permittivity of the expanded solvent, ε_{CO_2} is the dielectric for pure CO_2 at 50 bar, X_{CO_2} is the mole fraction of CO_2 in the expanded mixture, ε_{solv} is the dielectric of the pure liquid solvent, and X_{solv} is the mole fraction of liquid solvent in the expanded mixture. Hence, the data in Table 1 and Fig. 1 can be used to directly calculate CO_2 solubilities.

Fig. 2 and Table 1 show the calculated solubility of CO_2 in different expanded solvents using the dielectrometry technique, and this is the first time that this technique has been used to determine gas solubilities in liquids. Here, addition of CO_2 at 50 bar pressure shows a varying degree of solubility in the range of solvents studied. Most of the expanded solvents show high CO_2 solubility, typically in the 0.6–0.7 mole fraction range, with cyclohexane demonstrating the highest CO_2 solubility (75 mol%). For these solvents, these data illuminate a neglected but significant factor for GXLs; the polar constituent represents the *minor* component of the mixture. In this regard, GXLs are in fact more comparable to sc fluids than to a classical condensed liquid. In contrast, the solubility of CO_2 in the heavier alcohols was much lower, with the poorest solubility in *t*-butanol (0.251 mole fraction). Similar data were obtained for 5 of the solvents studied here by Lazzaroni *et al.*[29] Although the experimental conditions and the method of analysis were different, the same trends were obtained.

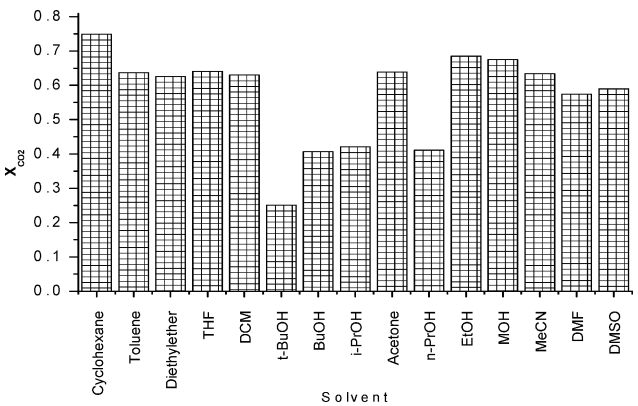

Fig. 2 Solubility of CO_2 at 50 bar pressure and 25 °C in a series of expanded solvents. Solvents are plotted in order of increasing dielectric polarity.

To determine a more accurate picture of a GXL it is important to quantify the change occurring in the molar volume upon expansion. Fig. 3 and Table 1 show the density of a range of organic solvents, plotted in order of increasing density at ambient pressure, and the degree to which their density changes when they are expanded under 50 bar of CO_2 at 25 °C. The

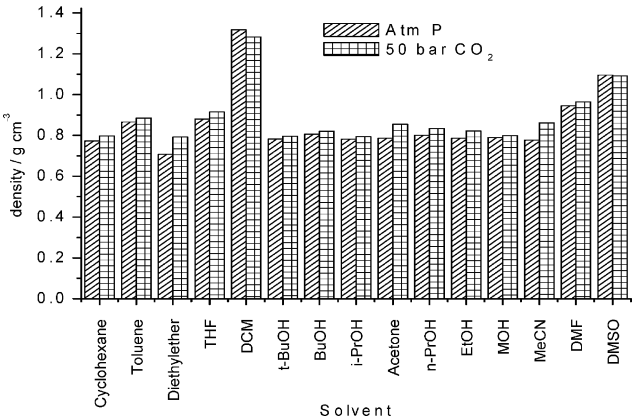

Fig. 3 Density data values for solvents at ambient pressure and for the CO_2 expanded equivalents at 50 bar pressure and 25 °C in order of increasing polarity.

density values were obtained with an uncertainty of ±2% and values obtained at ambient pressure were in good correlation with published data.[30] Significantly, there is no correlation between the solubility of CO_2 in these solvents and their density changes. For the majority of solvents, their densities increase on expansion with CO_2; *i.e.* CO_2 enters the void volume in the liquid molecules that are packed in a given volume, and only the more dense solvents, dichloromethane and dimethyl sulfoxide, showed a reduction in density. These data are entirely consistent with a previous study on the change in density as a function of pressure for five solvents, including dichloromethane,[14] where it was shown that the density of these solvents does not vary in a consistent manner with pressure. For each solvent, the density reaches a maximum, which interestingly occurs close to the critical pressure. This suggests that these maxima are related to overcoming the forces holding the solvent molecules together since p_c is the pressure required to liquefy a gas at T_c. At pressures above the maxima, further increases in CO_2 pressure result in an opposing effect where density begins to decrease. This density behaviour could be attributed to one or two different phenomena; liquid compression as a result of the application of pressure, or the solubilisation of CO_2 (or CO_2 occupying the void volume). However, analysis of the data in the form of density is slightly misleading, as CO_2 is a small but dense molecule and density measurements do not give a significant insight into liquid structure. A more useful analysis is to consider the molar volume of the liquid and determine what changes are happening to the free volume of the liquid upon expansion. The molar free volume, V_{free}, of a liquid can be determined from:

$$V_{free} = (M_w/\rho) - (N_A \times V) \quad (2)$$

where M_w is the molecular mass of the solvent, ρ is the density of the solvent at ambient pressure, N_A is Avogadro's constant, and V is the molecular volume.

Using the data presented in Fig. 3, V_{free} for the gas expanded liquid can also be calculated by carrying out the same procedure for each of the components of the mixture. Fig. 4 and Table 1 show that in contrast to the modest changes in density, gas expansion has a significant effect upon the percentage of the volume which is free. In general, the solvents that exhibit the

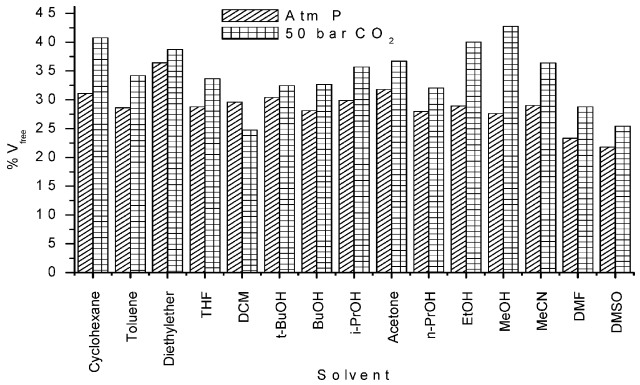

Fig. 4 Molar free volume in a variety of liquids together with the corresponding values for the same liquids expanded with CO_2 50 bar pressure at 25 °C.

largest solubilities for CO_2 show the greatest increases in molar free volume on expansion. This explains why the viscosities of these systems have been shown to be considerably lower than the corresponding unexpanded liquids.[31-33] This also shows that in terms of the free volume, all of these systems expand with the exception of DCM where the CO_2 fills the void volume rather than expanding the liquid lattice.

Fig. 5 shows that there is a direct correlation between this change in free volume and the mole fraction of CO_2 dissolved in the liquid for the protic solvents. The correlation is less marked for the non-hydrogen bonding solvents, with dichloromethane as the clear outlier. The linear correlation for protic solvents is to be expected, since as more CO_2 dissolves the hydrogen bonding structure of the solvent is disrupted and the free volume increases.

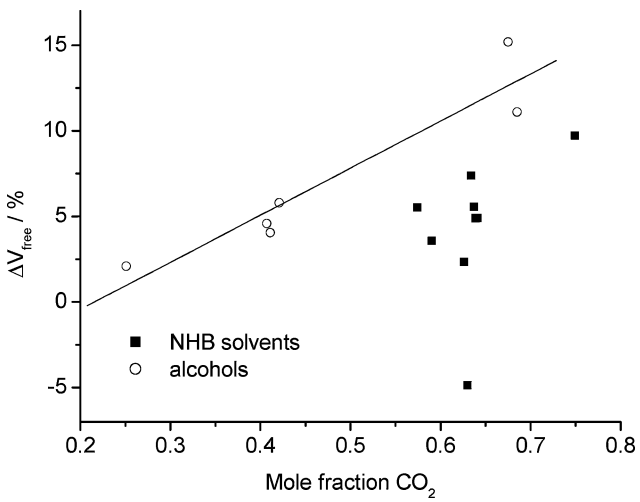

Fig. 5 Change in molar free volume upon pressurisation with solubility of CO_2 at 50 bar pressure and 25 °C.

The thermodynamics of CO_2 mixing depends upon the relative solvent–solute interactions. To dissolve CO_2 in the solvent it is necessary to overcome the intermolecular forces between the solute species (which should be negligible), the energy released when the CO_2 interacts with the solvent and the solvent–solvent interactions required to form a cavity for the solute. In a GXL it is the last of these that is likely to dominate, and this should be quantifiable using the Hildebrand solubility parameter, δ, in eqn (3).

$$\delta = \sqrt{\frac{\Delta H_{vap} - RT}{V_m}} \quad (3)$$

where ΔH_{vap} is the enthalpy of vaporisation and V_m is the molar volume of the pure solvent at 1 bar pressure. Fig. 6 clearly shows that there is a linear correlation between the change in molar free volume upon expansion and the Hildebrand solubility parameter confirming that the expansion of these molecular solvents is controlled by the thermodynamics of cavity formation. The density of most solvents only changes by a small amount, but in molar terms the free volumes of the expanded liquids can increase by over 10%. This, therefore, accounts for the considerably lower solubility of CO_2 in the higher alcohols which arises primarily from the stronger solvent–solvent interactions.

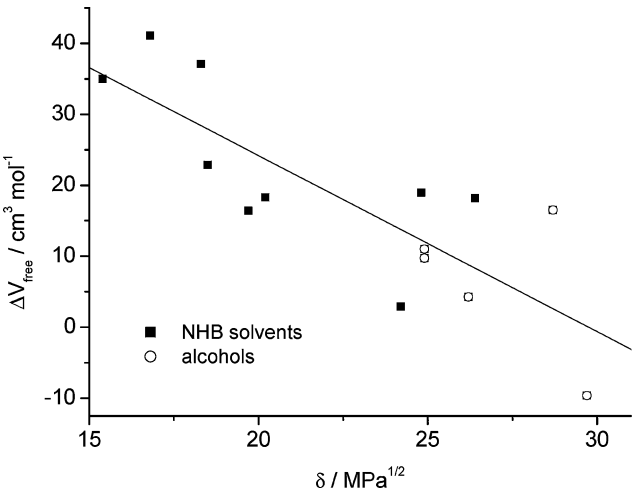

Fig. 6 Effect of the Hildebrand solubility parameter upon the change in molar free volume upon pressurisation at 50 bar CO_2 pressure and 25 °C.

Although relative permittivity and density data provide a measure of the bulk properties of a fluid, these only offer insight into average solvent properties. In contrast, the use of solvatochromic parameters allows an insight into solvation and local density, and has been particularly useful in an understanding of the solvent properties of supercritical fluids.[34–36] The two most commonly used scales are the $E_T(30)$ polarity scales of Dimroth and Reichardt[37] and the multi parameter scale of Kamlet and Taft.[38] The full Kamlet and Taft analysis of these data in this case is complex and dealt with in more detail elsewhere.[39] However in general the α and π^* values were obtained using Nile red and phenol blue as indicators. The spectral shifts obtained at ambient pressure were fitted with the literature values using multiple regression analysis with Microcal Origin 6.0. This resulted with the coefficients shown in eqn (4) and (5).

$$\text{Nile Red: } \nu_{max} = 19.9657 - 1.0241\pi^* - 1.6078\alpha \quad (4)$$

$$\text{Phenol Blue: } \nu_{max} = 18.2086 - 0.9990\pi^* - 1.4883\alpha \quad (5)$$

Table 1 lists the parameters at 50 bar of CO_2 and 25 °C. The data recorded for the solvents under ambient pressure conditions

Table 2 The change in polarisability/polarity parameter, π^*, and the hydrogen bond acceptor parameter, α, when various alcohols were exhibited to 50 bar CO_2 pressure at 25 °C

	π^* (1 bar)	π^* (50 bar)	Change π^*	α (1 bar)	α (50 bar)	Change α
MeOH	0.598	0.372	–0.226	0.925	0.638	–0.286
EtOH	0.537	0.291	–0.246	0.848	0.535	–0.313
n-PrOH	0.520	0.336	–0.183	0.825	0.593	–0.232
i-PrOH	0.482	0.346	–0.136	0.778	0.606	–0.173
n-BuOH	0.508	0.439	–0.069	0.810	0.723	–0.087
t-BuOH	0.407	0.373	–0.033	0.682	0.640	–0.042

showed a good correlation with those reported in the literature. The data also correlate well with the limited background literature for expanded systems with acetonitrile, methanol and acetone.[40,41] As expected the polarity parameters all decrease upon pressurisation, as the local cybotactic region becomes enriched with the less polar CO_2. However, no correlation exists between π^* or E_T and either the relative permittivity or the density (not shown). It has been shown previously that the reaction field, R, created by an electrostatic field of polar molecules surrounding a solute can be determined using

$$R = \frac{2(\varepsilon - 1)\mu_G}{(2\varepsilon + 1)a^3} \quad (6)$$

where; μ_G is the dipole moment of the solute in the ground state, and a is the radius of the cavity occupied by the solute. If the reaction field is accountable for the stabilisation of the excited state of the indicator solute then it is possible to correlate the Kirkwood function, $(\varepsilon - 1)/(2\varepsilon + 1)$ with π^*. Fig. 7 shows that there is a good correlation between these two parameters for the alcohols, however this is less valid for non-hydrogen bonding (NHB) solvents. As expected a strong correlation exists between the π^* and the Dimroth–Reichard E_T polarity scales and hence naturally between the E_T values and the Kirkwood function.

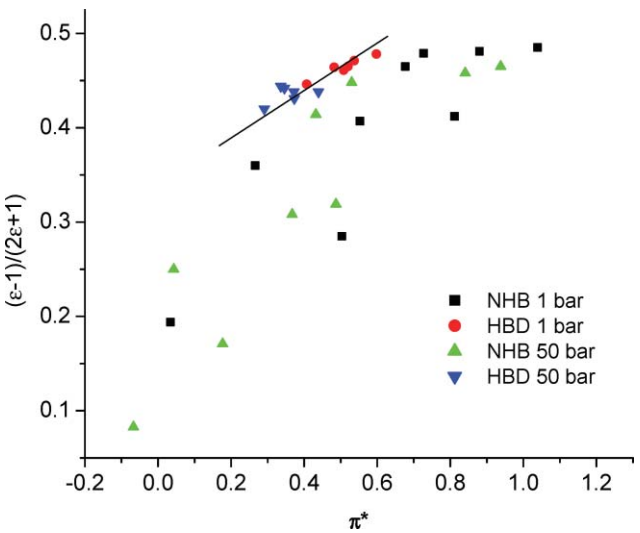

Fig. 7 Correlation between polarisability, π^*, and the Kirkwood function, $(\varepsilon - 1)/(2\varepsilon + 1)$. The solvents are classified as non-hydrogen bonding (NHB) and hydrogen bond donating (HBD).

The behaviour of the alcoholic liquids when pressurised with CO_2 could be explained in terms of the insertion of CO_2 into the alcohol and formation of the corresponding alkylcarbonic acid. The above results show that the alcohols behave in a similar manner to the other solvents, and alkylcarbonic acid that does form has only a minor effect on the overall physical properties of the mixture. This is reinforced by the recent study by Gohres *et al.* who showed that the equilibrium constant for the acid formation is still relatively small.[42]

If the local composition were simply related to the bulk composition then the polarity of the mixture would simply be related to the mole fraction in the bulk; *i.e.* for the π^* scale:

$$\pi^*_{mix} = X_{CO_2}\pi^*_{CO_2} + (1 - X_{CO_2})\pi^*_{solv} \quad (7)$$

However, for all fifteen solvents, the π^*_{mix} (expanded solvent) values are significantly larger than those predicted from the bulk CO_2 values in Table 2 and Fig. 2, demonstrating that preferential solvation of the solvatochromic probe by the more polar solvents occurs. This mirrors the observations in supercritical CO_2 with polar modifiers. Eqn (7) can also be used to calculate the local composition of solvent around the indicator solute (X_{local}). In supercritical fluids, the ratio of local to bulk densities decreases as the bulk density increases and this phenomenon is termed local density augmentation. This has been reviewed in a number of articles.[43,44] We have also shown that at constant reduced temperature X_{local}/X_{bulk} is approximately constant at a given reduced pressure.[45] In mixed fluids, the local concentration of the more polar constituent remains constant at lower pressures and decreases at higher pressure.[46] Recent work by Eckert *et al.* has applied this to selected GXLs.[47,48] Fig. 8 shows a X_{local}/X_{bulk} ratio

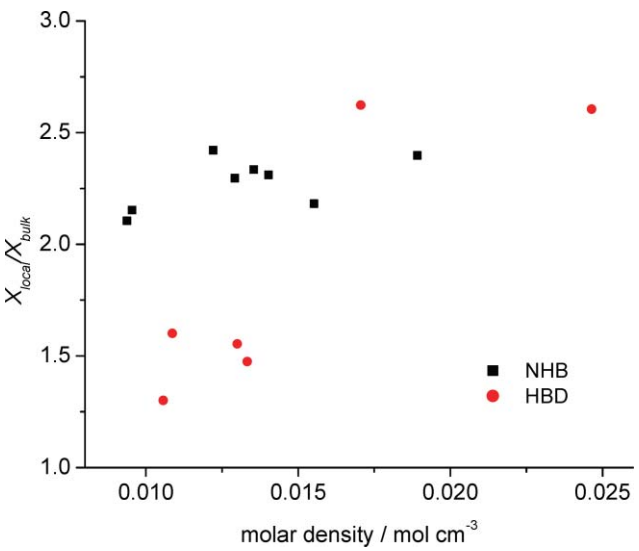

Fig. 8 Mole fraction of CO_2 in the local and bulk solvent as a function of molar density with 50 bar CO_2 at 25 °C and fixed volume.

of 2.3 for all solvents except the higher alcohols, which agrees well with the value found for acetonitrile.[47] This shows that the more polar constituent preferentially solvates the indicator solute. The constancy of the local solvation is unexpected but shows that there are clear similarities between the solvation in modified sc fluids and GXLs. It suggests that the equilibrium between species in the bulk and those in the cybotactic region are dominated by the overall system pressure rather than the absolute density.

Using the multi-parameter Kamlet and Taft scale it is possible to probe the effects of compression and substitution. It has been shown that for supercritical fluids compression of a medium has the opposing effects of increasing π^* while decreasing the hydrogen bond acceptor, α, properties. Table 2 lists the π^* and α values for the pure and CO_2 expanded alcoholic solvents. It can be seen that in all cases both parameters decrease upon pressurisation and a strong linear correlation exists ($r = 0.9996$) between the change in both polarity parameters, suggesting that the major effect in solvation is one of substitution rather than compression.

Conclusion

This work has provided a significant insight into the solution structure and solvation in GXLs. It has been shown that CO_2 solubility is relatively similar at 50 bar in a wide range of organic solvents (*ca.* 70 mol%) with the exception of higher alcohols where it is approximately half that value. The measurement of solvent density has shown that while the actual solvent density is relatively unaffected by pressurisation, the free volume of a liquid can increase by up to 10%, accounting for the solvent and transport properties of the fluids. The measurement of solvent polarity using solvatochromic indicator solutes has allowed an insight into solvation in GXLs to be obtained. This has shown that preferential solvation of the indicator solute occurs by the more polar solvent, which is analogous to the effects seen in modified supercritical fluids. Similarly, the amount of more polar species in the cybotactic region is approximately double that in the bulk.

Acknowledgements

We thank EPSRC (RM) and the Royal Society (AMS) for financial support.

References

1 L. C. Draucker, J. P. Hallett, D. Bush and C. A. Eckert, *Fluid Phase Equilib.*, 2006, **241**, 20.
2 K. N. West, J. P. Hallett, R. S. Jones, D. Bush, C. L. Liotta and C. A. Eckert, *Ind. Eng. Chem. Res.*, 2004, **43**, 4827.
3 M. Wei, G. T. Musie, D. H. Busch and B. Subramaniam, *J. Am. Chem. Soc.*, 2002, **124**, 2513.
4 P. G. Jessop, M. M. Olmstead, C. D. Ablan, M. Grabenauer, D. Sheppard, C. A. Eckert and C. L. Liotta, *Inorg. Chem.*, 2002, **41**, 3463.
5 C. A. Thomas, R. J. Bonilla, Y. Huang and P. G. Jessop, *Can. J. Chem.*, 2001, **79**, 719.
6 J. W. Tom and P. G. Debenedetti, *Biotechnol. Prog.*, 1991, **7**, 403.
7 C. J. Chang and A. D. Randolph, *AIChE J.*, 1989, **35**, 1876.
8 R. S. Mohamed, P. G. Debenedetti and R. K. Prudhomme, *AIChE J.*, 1989, **35**, 325.
9 D. W. Matson, R. C. Petersen and R. D. Smith, *J. Mater. Sci.*, 1987, **22**, 1919.
10 P. M. Gallagher, M. P. Coffey, V. J. Krukonis and N. Klasutis, *ACS Symp. Ser.*, 1989, **406**, 334.
11 S. D. Yeo, G. B. Lim, P. G. Debenedetti and H. Bernstein, *Biotechnol. Bioeng.*, 1993, **41**, 341.
12 T. W. Randolph, A. D. Randolph, M. Mebes and S. Yeung, *Biotechnol. Prog.*, 1993, **9**, 429.
13 E. Reverchon and G. Della Porta, *Pure Appl. Chem.*, 2001, **73**, 1293.
14 J. Bleich and B. W. Muller, *J. Microencapsulation*, 1996, **13**, 131.
15 E. Weidner, Z. Knez, and Z. Novak, *PGSS (Particles from Gas saturated Solutions) a new process for powder generation*, in *Proceedings of the Third International Symposium on Supercritical Fluids, Strasbourg, France 1994*, ed. G. Brunner and M. Perrut, vol. 3, p. 229, IBSN 2-905-267-23-8.
16 B. Subramaniam and M. A. McHugh, *Ind. Eng. Chem. Proc. Des. Dev.*, 1986, **25**, 1.
17 C. A. Eckert, B. L. Knutson and P. G. Debenedetti, *Nature*, 1996, **383**, 313.
18 P. G. Jessop and B. Subramaniam, *Chem. Rev.*, 2007, **107**, 2666.
19 J. C. Gjaldbaek and J. H. Hildebrand, *J. Am. Chem. Soc.*, 1949, **71**, 3147.
20 H. Hiraoka and J. H. Hildebrand, *J. Phys. Chem.*, 1964, **68**, 213.
21 J. H. Hildebrand and R. G. Linford, *J. Phys. Chem.*, 1969, **73**, 4410.
22 J. C. Gjaldbaek and H. Nieman, *Acta Chem. Scand.*, 1958, **12**, 611.
23 J. M. Prausnitz and F. H. Shair, *AIChE J.*, 1961, **7**, 682.
24 J. M. Prausnitz, *J. Phys. Chem.*, 1962, **66**, 640.
25 T. Katayama, M. Tomosaburo and T. Nitta, *Kagaku Kogaku*, 1967, **31**, 559.
26 A. Hourri, J. M. St-Arnaud and T. K. Bose, *Rev. Sci. Instrum.*, 1998, **69**, 2732.
27 A. P. Abbott, S. Corr, N. E. Durling and E. G. Hope, *J. Chem. Eng. Data*, 2002, **47**, 900.
28 G. Leeke, R. Santos, B. Al-Duri, J. Seville, C. Smith and A. B. Holmes, *J. Chem. Eng. Data*, 2005, **50**, 1370.
29 M. J. Lazzaroni, D. Bush, J. S. Brown and C. A. Eckert, *J. Chem. Eng. Data*, 2005, **50**, 60.
30 R. H. Perry and D. W. Green, *Chemical Engineers' Handbook*, 7th edn, McGraw-Hill, 1997.
31 Y. W. Kho, D. C. Conrad and B. L. Knutson, *Fluid Phase Equilib.*, 2003, **206**, 179.
32 R. Sih, F. Dehghani and N. R. Foster, *J. Supercrit. Fluids*, 2007, **41**, 148.
33 R. Sih, M. Armenti, R. Mammucari, F. Dehghani and N. R. Foster, *J. Supercrit. Fluids*, 2008, **43**, 460.
34 T. Sasaki, H. Takeishi and Z. Yoshida, *J. Supercrit. Fluids*, 1999, **15**, 23.
35 M. Maiwald and G. M. Schneider, *Ber. Bunsen-Ges. Phys. Chem.*, 1998, **102**, 960.
36 C. R. Yonker and R. D. Smith, *J. Phys. Chem.*, 1988, **92**, 235.
37 C. Reichardt, *Chem. Rev.*, 1994, **94**, 2319.
38 M. E. Jones, R. W. Taft and M. J. Kamlet, *J. Am. Chem. Soc.*, 1977, **99**, 8452.
39 R. Mistry, *PhD. Thesis*, University of Leicester, 2008.
40 J. W. Ford, J. Lu, C. L. Liotta and C. A. Eckert, *Ind. Eng. Chem. Res.*, 2008, **47**, 632.
41 V. T. Wyatt, D. Bush, J. Lu, J. P. Hallett, C. L. Liotta and C. A. Eckert, *J. Supercrit. Fluids*, 2005, **36**, 16.
42 J. L. Gohres, A. T. Marin, J. Lu, C. L. Liotta and C. A. Eckert, *Ind. Eng. Chem. Res.*, 2009, **48**, 1302.
43 S. C. Tucker, *Chem. Rev.*, 1999, **99**, 391.
44 J. F. Brennecke and J. E. Chateauneuf, *Chem. Rev.*, 1999, **99**, 433.
45 A. P. Abbott and C. A. Eardley, *J. Phys. Chem. B*, 1999, **103**, 2504.
46 A. P. Abbott, C. A. Eardley and J. E. Scheirer, *J. Phys. Chem. B*, 1999, **103**, 8790.
47 J. W. Ford, M. E. Janakat, J. Lu, C. L. Liotta and C. A. Eckert, *J. Org. Chem.*, 2008, **73**, 3364.
48 J. L. Gohres, C. L. Kitchens, J. P. Hallett, A. V. Popov, R. Hernandez, C. L. Liotta and C. A. Eckert, *J. Phys. Chem. B*, 2008, **112**, 4666.